Available online at www.sciencedirect.com

ScienceDirect

Procedia Engineering 172 (2017) 1059 – 1066

Procedia Engineering

www.elsevier.com/locate/procedia

Modern Building Materials, Structures and Techniques, MBMST 2016

Incremental Displacement Collocation Method for the Evaluation of Tension Softening Curves of Quasi-brittle Materials

R.K.L. Su[a,*], Q.F. Liu[a]

[a] *Department of Civil Engieering, The University of Hong Kong, Pokfulam Road, Hong Kong, 999077, China*

Abstract

In this paper, the use of incremental displacement collocation method (IDCM) for the evaluation of the tension softening curve of quasi-brittle materials is presented. By varying the residual tensile stress on the tension softening curve (TSC) for each loading step, the measured displacements are matched with the computed displacements at selected locations. By gradually increasing the loading step, the complete TSC can be determined in a step-by-step manner. As distinct global and local deformation responses are employed in the IDCM, the ill-posed problem commonly encountered in other inverse analyses is avoided. The effectiveness of the IDCM is demonstrated by obtaining TSCs of quasi-brittle materials, such as mortar, concrete and graphite, in the forms of bilinear, tri-linear and exponential curves.

Keywords: Tension softening curve; quasi-brittle; finite element; displacement field; inverse analysis.

1. Introduction

Concrete, mortar, graphite are all belongs to quasi-brittle materials. They are good at resisting compression but weak in tension. Linear elastic fracture mechanics (LEFM) is not applicable to quasi-brittle materials as stress singularity does not really exist at the crack tip. Nonlinear fracture mechanics (NLFM) should be used to analyse quasi-brittle materials.

In recent decades, many efforts have been made to the nonlinear fracture analysis of quasi-brittle materials [1-11]. Among these efforts, cohesive crack model (CCM) is extensively used to simulate the fracture behaviour of nonlinear fracture zone, which is so-called fracture process zone (FPZ). According to the CCM, all the nonlinear behaviours in the FPZ are represented by a cohesive crack, and the crack propagation is determined by the tension

* Corresponding author. Tel.: +852 2859 2648; fax: +852 2559 5337.
E-mail address: klsu@hkucc.hku.hk.

Peer-review under responsibility of the organizing committee of MBMST 2016
doi:10.1016/j.proeng.2017.02.163

softening curve (TSC).

Some researchers [1-3] attempted to obtain the TSC of concrete from uniaxial tension tests. However, as the crack path may not be known a priori or the crack propagation may not be stable and symmetrical, it is difficult to accurately estimate the TSC from the test, and only the average cohesive stress and crack opening can be obtained [4]. Alternatively, inverse analyses were proposed to evaluate the TSC by minimizing the difference between the numerical results and experimental response using optimization algorithms [5-7]. The shapes of TSC are assumed to be linear [8], bilinear, tri-linear [9] or exponential [10,11]. Kitsutaka [12] and Kurihara et al. [13] proposed a polylinear softening model without a prior assumption on the shape of the TSC. It is noted that all these inverse analysis approaches only consider the global response such as load-deflection and load-CMOD curve but not the local response near the crack. Shen and Paulino [14] proposed a hybrid inverse technique and employed the local responses at one loading state in the post-peak stage of the beam. Skoček and Stang [15] used optical method to measure the displacements and performed wedge splitting tests to inversely estimated the fracture parameters, assuming the softening curve is piecewise and linear. Although optimization algorithms were utilized in the numerical analysis, ill-posed problems were commonly found in the aforementioned inverse analysis.

In this paper, a recently developed incremental displacement collocation method (IDCM) [16-18] is presented for the estimation of the TSCs of quasi-brittle materials in a step-by-step manner. At each numerical step, an assumed trial cohesive stress is used along with the measured global and local response, including the length of FPZ, to predict the TSC. The trial cohesive stress is determined by matching the displacements measured from experiment using electronic speckle pattern interferometry (ESPI) technique and that from the finite element (FE) analysis. Using the IDCM, the ill-posed problem is suppressed and the TSCs of mortar [16], concrete [17] and graphite [18] are determined.

2. Theoretical background of IDCM

2.1. Basic assumptions

To determine the TSC with IDCM [16], which is facilitated by incorporating CCM into the finite element method (FEM), the following assumptions are adopted:

(1) A two-dimensional crack model is employed.
(2) The nonlinear fracture behaviour is represented by a cohesive crack ahead of the notch tip
(3) The remaining parts of the specimen are assumed to be isotropic and linear elastic.
(4) The cohesive crack starts to propagate when the maximum tensile stress equals to the tensile strength.
(5) The trial cohesive stress follows a decreasing trend as the crack opening increases.
(6) The cohesive stresses in the FPZ are determined by the extended TSC and the measured crack opening displacement (COD).

2.2. The CCM

As shown in Fig. 1, the nonlinear behaviour of all the crack regions in the CCM is represented by TSC which relates the cohesive stress σ with the crack opening w in the FPZ. From Fig. 1b and c, the following boundary conditions for $\sigma = f(w)$ should be satisfied:

$$w = w_c,\ \sigma = 0;\ w = 0,\ \sigma = f_t. \tag{1}$$

For a cohesive crack with its front and rear ends at the locations $x=x_2$ and $x=x_1$, respectively, the length of the cohesive crack is

$$l_p = x_2 - x_1. \tag{2}$$

Because the crack opening w at all locations can be obtained directly from the experimental COD profile, the length of the FPZ can be determined with IDCM. Once the piecewise-linear relationship of the TSC has been defined, the cohesive stress distribution within the FPZ can be evaluated.

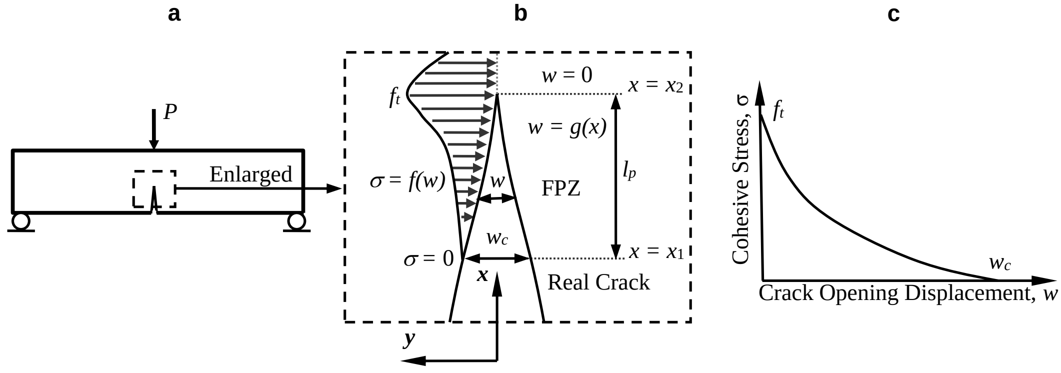

Fig. 1. (a) Sketch of a crack configuration. (b) Sketch of a cohesive crack. (c) Cohesive law [16].

3. IDCM methodology

3.1. FEM

The three point bend test was simulated using the FEM. According to the symmetry of the specimen, only one half of the beam was analyzed. The specimen configuration and FE meshes are illustrated in Fig. 2 as an example. In the IDCM, the Young's modulus E is determined using FEM by comparing the simulated and experimental displacements. The Poisson's ratio ν was taken as 0.2.

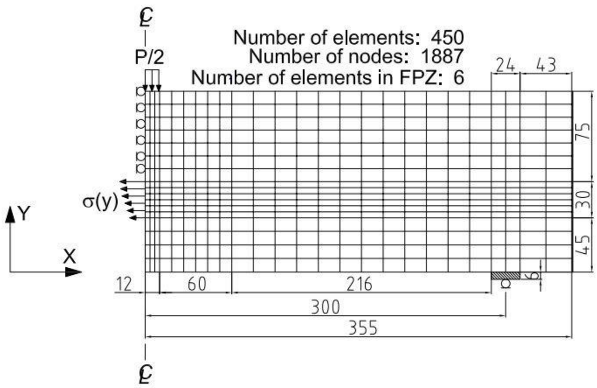

Fig. 2. Specimen configuration and FE meshes (unit: mm) [17].

2.1.2. Procedure of the IDCM

Both the global responses, such as the load-deflection and load-CMOD curves, and the local responses, including the complete COD profile, the location of crack front (x_2) and hence l_p at each of the loading steps, are determined by the ESPI technique. By matching displacements from the FE analysis and experiments at various collocation points, the piecewise-linear relationship of the TSC and the Young's modulus E of the material can be evaluated. In this method, the TSC is determined in a step-by-step manner as shown in Fig. 3, and the details are described herein.

First, the experimental displacements, including mid-span deflection δ, CMOD, NTOD and the COD profile, are extracted with the ESPI technique and used in the numerical analysis.

Second, the ultimate tension strength f_t are determined inversely at the early loading stages or obtained from the splitting tension test. At the early loading stage, the crack is small and the length of FPZ is short. The cohesive stress in the FPZ can be assumed to be uniformly distributed and equal to f_t. Then the Young's modulus E can be determined with FEM by matching the calculated and measured displacements in the linear elastic deformation stage.

Third, in the COD profile, the positions of the front of the crack and the rear end of the cohesive crack (e.g., the initial notch tip) are identified; thus, the length of the FPZ can be determined. In the FPZ, cohesive stresses will be assigned to the interfacial elements along the crack line.

Fourth, from the COD profile, the crack opening $w(y)$ can be determined at various interfacial nodes in the FPZ of the FEM data set. The y axis is defined along the crack line with the origin at the notch mouth. As shown in **Error! Reference source not found.**a, at the i^{th} loading step, all of the nodal points on the TSC in the previous i-1th loading steps would have been defined; only the last step (w_i, σ_i) needs to be determined using the IDCM. The cohesive stresses at all the interfacial nodes with w less than or equal to w_{i-1} can then be established. Because the TSC must be a decreasing function, the unknown stress σ_i should satisfy the following requirement:

$$\sigma_i \le \sigma_{i-1} \tag{3}$$

where σ_{i-1} is the cohesive stress determined at the i-1th loading step. For $i=1$, σ_0 is equal to f_t, which can be determined by the splitting tension test.

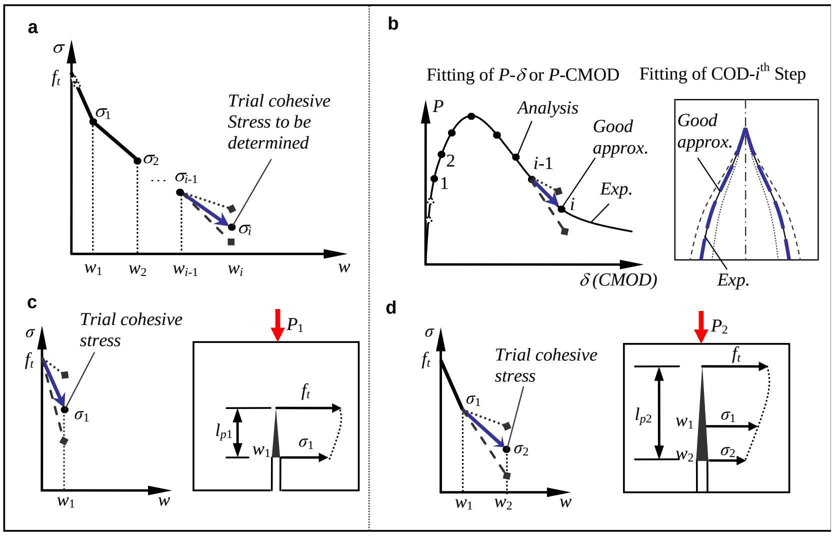

Fig. 3. The principle of the IDCM: (a) incremental construction of the TSC; (b) displacement collocation for the estimation of the trial stress; (c) estimation of the 1st trial stress σ1; (d) estimation of the 2nd trial stress σ_2 [16].

Using linear interpolation, the nodal cohesive stress $\sigma(y)$ at the j^{th} segment of the TSC can be expressed in terms of the crack opening:

$$\sigma(y) = \sigma_{j-1} + \frac{\sigma_j - \sigma_{j-1}}{w_j - w_{j-1}}(w(y) - w_{j-1}) \tag{4}$$

where $w(y)$ is the crack opening of the node considered; (w_{j-1}, σ_{j-1}) and (w_j, σ_j) are the end coordinates of the j^{th} line segment; ($w(y)$, $\sigma(y)$) is a point on the line segment; and j = 1, 2,…i. By assigning a certain trial value for σ_i that satisfies Equation (2), and using Equation (3), all of the nodal stresses along the FPZ can be obtained.

Lastly, the nodal cohesive stress σ_i is accepted only when two additional requirements, displacement and stress, are satisfied as follows. The displacement requirement is

$$| d_n - d_e | < \text{Tolerance} \tag{5}$$

where d_n and d_e represent the calculated and measured displacements, respectively, in terms of δ, CMOD and NTOD (Fig. 3b).

For the stress requirement, the calculated stresses in the relevant domain should not be greater than f_t, and the numerical stress profile in the FPZ should be a smooth curve. Prior to the formation of a fully developed FPZ, all nodal cohesive stresses should be greater than zero. It can then proceed to the next loading step. The above procedure is repeated until the crack opening at the initial notch tip reaches w_c and σ_i=0.

4. Results and discussion

4.1. Specimens

Two central-notched mortar beams (Unit 1 and Unit 2), five batches of concrete samples (C40 to C90) and two types of graphites (IG11 Series and NG-CT-01 Series) were tested to evaluate their TSCs. Parameters of the central-notched specimen are shown in Table 1. After being cast and cured, the mortar and concrete specimens were placed in air (temperature: 20±2°C; relative humidity: 75-85%) until the date of testing. The cube compressive strength f_{cu}, the static modulus of elasticity in compression E_c and the splitting tensile strength f_{st} were obtained according to the Hong Kong construction standard.

Table 1. Parameters of the central-notched beams.

Materials	Maximum size of aggregate (mm)	Initial notch depth (mm)	Width of the notch (mm)	Specimen size (mm)	Span of the beam (mm)	f_{cu} (MPa)	f_{st} (MPa)
Mortar	5	30	3	500 × 100 × 40	400	29.5	2.25
Concrete	10	45	3	710 × 150 × 80	600	39.7-86.7	2.5-5.4
IG11		20	0.5	220 × 50 × 25	200	78	25
NG-CT-01		20	0.5	220 × 50 × 25	200	76	24

4.2. The TSC of mortar

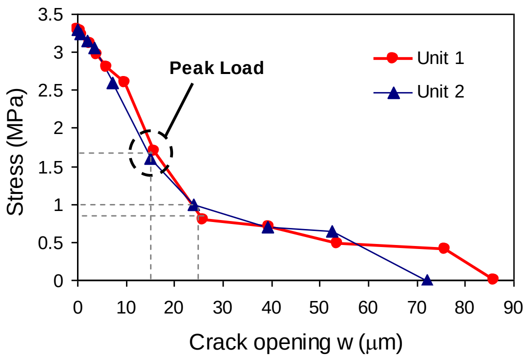

Fig. 4. TSC of mortar obtained from the IDCM [16].

Using IDCM, the estimated TSCs for both specimens are shown in Fig. 4. The characteristic crack openings w_c for Units 1 and 2 are 72.9 μm and 87.5 μm, respectively. The ratio of $w_c \cdot f_t$ to the fracture energy G_F (81.78 N/m) is approximately 3.24.

It is found that, at the peak load, the cohesive stresses at the initial notch tip are about 1.65 MPa ($0.5f_t$) and the corresponding crack opening w is 15 μm. When w increases from zero to 25 μm, the cohesive stresses drop quickly from f_t to 0.8 MPa for Unit 1 and 1 MPa for Unit 2, which correspond to $0.25f_t$ and $0.33f_t$ respectively. From that point, the stress decreases gradually until w increases to 75 μm for Unit 1 and 60 μm for Unit 2 and the stress decreases rapidly to zero. Referring to the aforementioned assumptions on the shape of the TSC, such as linear, bi-linear, tri-linear and exponential curves, a tri-linear curve was found to be the best approximation of mortar.

4.3. The TSC of concrete

To facilitate future simulations of concrete fractures using commercial finite element packages, the TSCs identified in the current study were simplified to bilinear and exponential curves using regression analysis, as shown in Fig. 5. The basic parameters used to define the TSC, including the total fracture energy G_F and the critical crack opening displacement w_c, were obtained using inverse analysis. The tensile strength was obtained from the splitting tension test or the inverse analysis. In addition to these parameters, parameters are determined for each individual curve. The critical parameter for a bilinear curve is the location of the kink point (w_1, f_1), see Fig. 5a. The exponential curve was derived empirically by Hordijk [19], see Fig. 5b. The function is expressed as

$$\sigma / f_t = \left\{1+\left(c_1 w / w_c\right)^3\right\} \exp\left(-c_2 w / w_c\right) - w / w_c \left(1+c_1^{\,3}\right) \exp(-c_2) \tag{6}$$

$$w_c = c_3 G_F / f_t \tag{7}$$

where c_1, c_2 and c_3 are the parameters of the exponential curves to be determined for concrete.

A complete set of parameters for defining the bilinear and exponential curves are listed in Table 2. To compare the modelling effect of the idealised curves, the root-mean-square deviation (RMSD) was evaluated, as presented in Table 2. For concrete with compressive strength $f_{cu} \le 60$ MPa, the bilinear curve can model the TSCs fairly accurately, while for C80 and C90 concrete, the RMSD of bilinear fitting is statistically significant. For bilinear fitting, the stress ratio f_1/f_t at the kink point varies within 0.21-0.28. Exponential curves can provide satisfactory approximations for the TSCs of all concrete strengths.

Table 2. Parameters of the idealised TSC curves [17].

Series	Fracture parameters			Bilinear curve					Exponential curve			
	G_F (N/m)	w_c (μm)	f_t (MPa)	w_1 (μm)	f_1 (MPa)	w_1/w_c	f_1/f_t	RMSD	c_1	c_2	c_3	RMSD
C40	96.4	214.0	2.5	22.9	0.7	0.11	0.28	0.075	6.0	1.5	5.6	0.201
C50	120.1	184.3	2.9	42.0	0.7	0.23	0.23	0.089	6.5	1.8	5.8	0.047
C60	129.6	238.3	3.3	33.0	0.7	0.14	0.21	0.137	7.9	2.9	6.1	0.108
C80	124.2	188.7	4.5	20.3	1.0	0.11	0.22	0.262	11	5.0	6.8	0.146
C90	114.6	165.0	5.4	12.0	1.2	0.07	0.22	0.258	13	6.0	7.2	0.187

To ease the estimation of the fracture properties of concrete, the parameters for defining an exponential TSC were related to the compressive strength f_{cu}. Empirical equations for c_1, c_2 and c_3 were expressed in terms of f_{cu} that ranges from 40 MPa to 90 MPa and the typo-errors originally occurred in Ref [17] have been corrected.

$$c_1 = 0.431 \exp(0.0304 f_{cu}) \tag{8}$$

$$c_2 = 2.965\exp(0.0165 f_{cu}) \quad (9)$$

$$c_3 = 4.486\exp(0.0053 f_{cu}) \quad (10)$$

From the empirical formulas, the parameters of the exponential TSC seem only rely on the compressive strength. However, it should be noted that the tensile properties of concrete are dependent on the physical properties of the material, e.g. aggregate size, and the size of the tested specimen. With comparable aggregate size and specimen size, current empirical formulas are feasible to estimate the TSC from the compressive strength even for concrete with compressive strengths outside the range of 40-90 MPa.

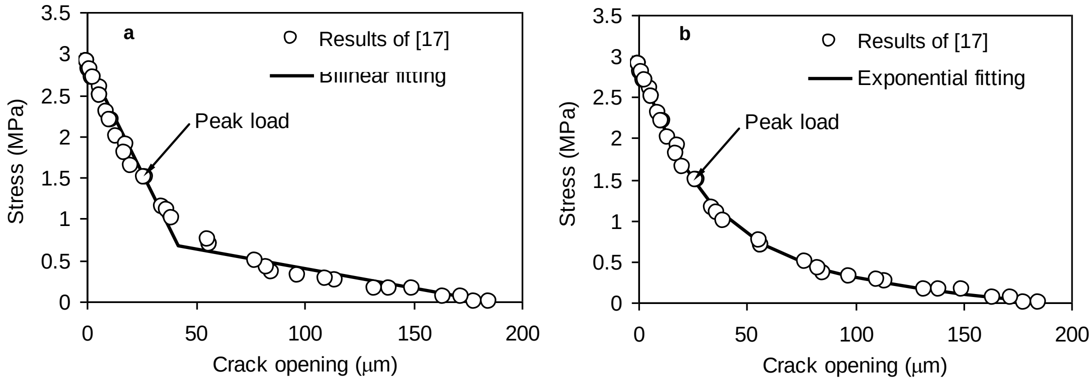

Fig. 5. Approximations of the estimated TSCs: (a) bilinear fitting; (b) exponential fitting [17].

4.4. The TSC of graphite

Similar to concrete, the TSC of graphite can also be simplified to be bilinear, tri-linear and exponential curves. A complete set of parameters for defining the bilinear, tri-linear and exponential curves is listed in Table 3. All the idealised curves could provide a satisfactory approximation for the TSCs if the initial descent of the TSC was not too sharp. However, when the tensile strength is high and the cohesive stress drops suddenly in the initial region of the TSC, only the tri-linear curve can accurately capture the abrupt change. Thus, the tri-linear curve is the best for fitting the TSC of nuclear graphite.

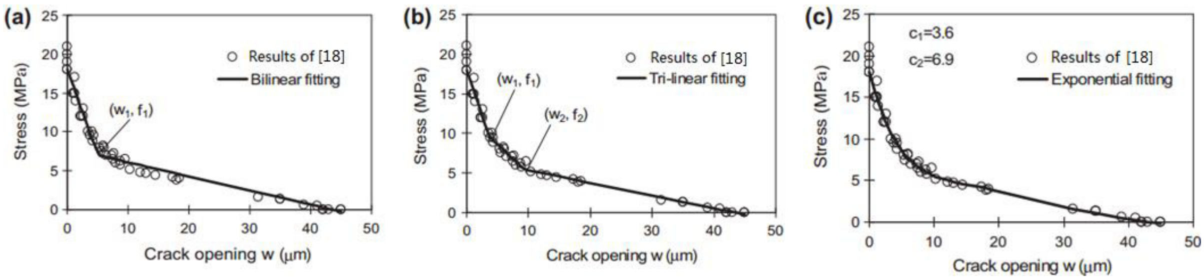

Fig. 6. Approximations of the TSC estimated: (a) bilinear fitting; (b) tri-linear fitting; (c) exponential fitting [18].

Conclusions

The assumptions and formulation of IDCM have been described in detail. The effectiveness of the method is revealed by determining the TSCs of various quasi-brittle materials in the forms of bilinear, tri-linear and exponential functions.

Table 3. Parameters of the idealised TSC curves of graphite [18].

Series	Fracture parameters		Bilinear curve		Tri-linear curve				Exponential curve		
	G_F (N/m)	f_t (MPa)	w_1 (μm)	f_1 (MPa)	w_1 (μm)	f_1 (MPa)	w_2 (μm)	f_2 (MPa)	c_1	c_2	c_3
IG11	192.1	18.2	5.1	7.0	4.7	8.3	11.1	5.0	3.6	6.9	4.1
NG-CT-01	180.2	19.4	3.7	6.8	2.5	9.5	10.2	4.4	3.8	7.5	5.3

References

[1] S.K. Lee, S.K. Woo, Y.C. Song, Softening response properties of plain concrete by large-scale direct tension tests, Mag. Concrete Res. 60 (2008) 33–40.

[2] V.S. Gopalaratnam, S.P. Shah, Softening response of plain concrete in direct tension, ACI Journal 82 (1985) 310–323.

[3] T.J. Boone, P.A. Wawrzynek, A.R. Ingraffea, V.S. Gopalaratnam, S.P. Shah, Softening response of plain concrete in direct tension, ACI Journal 83 (1986) 316–318.

[4] H.A.W. Cornelissen, D.A. Hordijk, H.W. Reinhardt, Experimental determination of crack softening characteristics of normalweight and lightweight concrete, Heron 31 (1986) 45–56.

[5] M. Elices, C. Rocco, C. Rosello, Cohesive crack modelling of a simple concrete: Experimental and numerical results, Eng. Fract. Mech. 76 (2009) 1398–1410.

[6] F.H. Wittmann, K. Rokugo, E. Brühwiler, H. Mihashi, P. Simonin, Fracture energy and strain softening of concrete as determined by means of compact tension specimens, Mater. Struct. 21 (1988) 21–32.

[7] J.L.A. De Oliveira, R. Gettu, Determining the tensile stress-crack opening curve of concrete by inverse analysis, J. Eng. Mech. 132 (2006) 141–148.

[8] A. Hillerborg, M. Modéer, P.E. Petersson, Analysis of crack formation and crack growth in concrete by means of fracture mechanics and finite elements, Cem. Concr. Res. 6 (1976) 773–781.

[9] B.M. Liaw, F.L. Jeang, J.J. Du, N.M. Hawkins, A.S. Kobayashi, Improved nonlinear model for concrete fracture, J. Eng. Mech. 116 (1990) 429–445.

[10] R.M.L. Foote, Y.W. Mai, B. Cotterell, Crack-growth resistance curves in strain-softening materials, J. Mech. Phys. Solids 34 (1986) 593–607.

[11] H.W. Reinhardt, Crack softening zone in plain concrete under static loading, Cem. Concr. Res. 15 (1985) 42–52.

[12] Y. Kitsutaka, Fracture parameters by polylinear tension-softening analysis, J. Eng. Mech. 123 (1997) 444–450.

[13] N. Kurihara, M. Kunieda, T. Kamada, Y. Uchida, K. Rokugo, Tension softening diagrams and evaluation of properties of steel fiber reinforced concrete, Eng. Fract. Mech. 65 (2000) 235–245.

[14] B. Shen, G.H. Paulino, Direct extraction of cohesive fracture properties from digital image correlation: a hybrid inverse technique, Exp. Mech. 51 (2011) 143–163.

[15] J. Skocek, H. Stang, Application of optical deformation analysis system on wedge splitting test and its inverse analysis, Mater. Struct. 43 (2010) 63–72.

[16] R.K.L. Su, H.H. Chen, A.K.H. Kwan, Incremental displacement collocation method for the evaluation of tension softening curve of mortar, Eng. Fract. Mech. 88 (2012) 49–62.

[17] H.H. Chen, R.K.L. Su, Tension softening curves of plain concrete, Constr. Build. Mater. 44 (2013) 440–451.

[18] R.K.L. Su, H.H. Chen, S.L. Fok, H. Li, G. Singh, L. Sun, L. Shi, Determination of the tension softening curve of nuclear graphites using the incremental displacement collocation method, Carbon 57 (2013) 65–78.

[19] D.A. Hordijk, Local approach to fatigue of concrete, Delft University of Technology, Ph.D. dissertation, 1991.